Research Article

Molecular Modeling of 2-Ethoxybenzonitrile dye sensitizer for solar cells using Quantum Chemical calculations

PM. Anbarasan[1]*, A. Prakasam[2] and P. Sakthivel[2]

[1]Centre for Nanoscience & Nanotechnology, Periyar University, Salem, Tamil Nadu, India.
[2]Department of Physics, Periyar University, Salem, Tamil Nadu, India.

ABSTRACT
The geometries, electronic structures, polarizabilities, and hyperpolarizabilities of organic dye sensitizer 2-Ethoxybenzonitrile was studied based on ab initio HF and Density Functional Theory (DFT) using the hybrid functional B3LYP. Ultraviolet-visible (UV-Vis) spectrum was investigated by Time Dependent DFT (TDDFT). Features of the electronic absorption spectrum in the visible and near-UV regions were assigned based on TDDFT calculations. The absorption bands are assigned to $\pi \rightarrow \pi^*$ transitions. Calculated results suggest that the three excited states with the lowest excited energies in 2-Ethoxybenzonitrile is due to photoinduced electron transfer processes. The interfacial electron transfer between semiconductor TiO_2 electrode and dye sensitizer 2-Ethoxybenzonitrile, is due to an electron injection process from excited dye to the semiconductor's conduction band. The role of nitro group in 2-Ethoxybenzonitrile in geometries, electronic structures, and spectral properties were analyzed.

Keywords: Dye sensitizer; Density functional theory; Electronic structure; Absorption spectrum.

1. INTRODUCTION

Because of the depletion of fossil fuels, growing demand of energy, global warming and other environmental problems, the development of environmental friendly renewable energy technologies is an urgent task for our human being[1]. Among all the renewable energy technologies, the nanocrystalline dye-sensitized solar cell (DSSC) system, a kind of photovoltaic device that presented by O'Regan and Gratzel in 1991, has attracted a lot of attention because of the potential application for low-cost solar electricity[2–5]. The main parts of DSSC are mesoporous oxide semiconductor layers that composed of nanoparticles and monolayer of dye sensitizers that attached to the surface of the semiconductor nano-films[3]. The dye sensitizers play an important role in DSSC that have a significant influence on the photoelectric conversion and transport performance of electrode[6–9]. Up to now, two kinds of dye sensitizers, which are generally known as metal-organic complexes and metal-free organic dyes, were studied extensively. In metal-organic complexes, especially the noble metal ruthenium polypyridyl complexes, including N3 and black dye etc. that were presented by Gratzel et al., have proved to be the best dye sensitizers with overall energy conversion efficiency greater than 10% under air mass (AM) 1.5 irradiation[10–12]. However, the limited metal Ru will become a bottleneck of application if the DSSC is widely used in our daily living[13]. On the other hand, metal-free organic dyes as sensitizers for DSSC, including cyanines, hemicyanines, triphenylmethanes, perylenes, coumarins, porphyrins, squaraines, indoline, and azulene- based dyes etc., have also been developed because of their high molar absorption coefficient, relatively simple synthesis procedure, various structures and lower cost[14–16]. In contrast to the numerous experimental studies of dye sensitizers, the theoretical investigations are relatively limited. Only several groups focused on the electronic structures and absorption properties of dye sensitizers [17–26], and Ru-complexes and organic dyes coupled TiO2 nanocrystalline[27–30], as well as the electron transfer dynamics of the

interface between dyes and nanocrystalline[31–35]. Until now, it remains a severe challenge for both experiment and theory to elucidate the fundamental properties of the ultrafast electron injection[30], and to approach the satisfied efficiency of DSSC. Further developments in dye design will play a crucial part in the ongoing optimization of DSSC[36], and it depends on the quantitative knowledge of dye sensitizer. So the theoretical investigations of the physical properties of dye sensitizers are very important in order to disclose the relationship among the performance, structures and the properties, it is also helpful to design and synthesis novel dye sensitizers with higher performance. Recently a rapid progress of organic dyes has been witnessed reaching close to 10.0% efficiencies in combination with a volatile acetonitrile-based electrolyte[37]. Nitrile is an important class of high performance dyes, which are easily processable, and display good mechanical properties, outstanding thermal and thermal-oxidative stability. Nitrile dyes were used for aerospace, marine, and electronic packaging applications by thermal treatment of nitrile derivatives at elevated temperatures (generally high up to 350 °C) for an extended period of time. In this paper the performance of 2-Ethoxybenzonitrile metal free dye that can be used in DSSC is analyzed.

2. Computational methods

The computations of the geometries, electronic structures, polarizabilities and hyperpolarizabilities, as well as electronic absorption spectrum for dye sensitizer 2-Ethoxybenzonitrile was done using ab initio HF and DFT with Gaussian03 package[38]. The DFT was treated according to Becke's three parameter gradient-corrected exchange potential and the Lee-Yang-Parr gradient-corrected correlation potential (B3LYP)[39–41], and all calculations were performed without any symmetry constraints by using polarized split-valence 6-311G(d,p) basis sets. The electronic absorption spectrum requires calculation of the allowed excitations and oscillator strengths. These calculations were done using TDDFT with the same basis sets and exchange-correlation functional in vacuum and solution, and the non-equilibrium version of the polarizable continuum model (PCM)[42,43] was adopted for calculating the solvent effects.

3. RESULTS AND DISCUSSION

3.1. The geometric structure

The optimized geometry of the 2-Ethoxybenzonitrile is shown in Fig.1, and the bond lengths, bond angles and dihedral angles are listed in Table 1. Since the crystal structure of the exact title compound is not available till now, the optimized structure can be only be compared with other similar systems for which the crystal structures have been solved. From the theoretical values we can find that most of the optimized bond lengths, bond angles and dihedral angles. The optimized bond lengths of C2-C3 and C3-C4 is 1.4141and 1.398 Å respectively at B3LYP/6-311G (d,p) and also well matched with HF/6-311G (d,p).

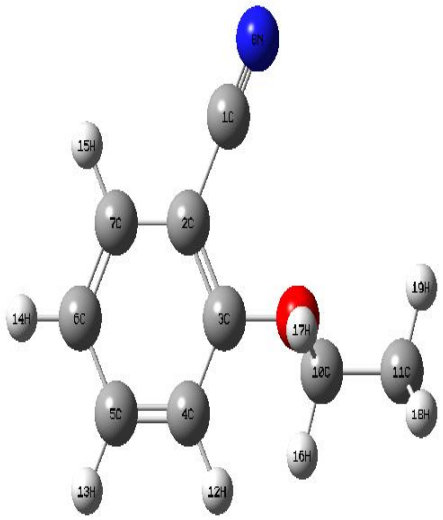

Fig. 1: Optimized geometrical structure of dye 2-Ethoxybenzonitrile

3.2. Electronic structures and charges

Natural Bond Orbital (NBO) analysis was performed in order to analyze the charge populations of the dye 2-Ethoxybenzonitrile. Charge distributions in C, N and H atoms were observed because of the different electro-negativity, the electrons transferred from C atoms to C, N

atoms, C atoms to H. The natural charges of different groups are the sum of every atomic natural charge in the group. These data indicate that the cyanine and amide groups are acceptors, while the acetic groups are donors, and the charges were transferred through chemical bonds. The frontier molecular orbitals (MO) energies and corresponding density of state of the dye 2-Ethoxybenzonitrile is shown in Fig. 2. The HOMO–LUMO gap of the dye 2-Ethoxybenzonitrile vacuum is 4.37 eV.

Table 1: Bond lengths (in Å), bond angles (in degree) and dihedral angles (in degree) of the dye 2-Ethoxybenzonitrile

Parameters	B3LYP/6-11++G(d,p)	HF/6-311++G(d,p)
Bond length(Å)		
C1-C2	1.4283	1.4412
C1-N8	1.1558	1.1309
C2-C3	1.4141	1.3924
C2-C7	1.3999	1.3919
C3-C4	1.3980	1.3858
C3-O9	1.3502	1.3473
C4-C5	1.3940	1.3828
C4-H12	1.0810	1.0744
C5-C6	1.3928	1.3878
C5-H13	1.0842	1.0753
C6-C7	1.3900	1.3798
C6-H14	1.0828	1.0742
C7-H15	1.0831	1.0744
O9-C10	1.4356	1.4222
C10-C11	1.5156	1.5118
C10-H16	1.0961	1.0868
C10-H17	1.0961	1.0856
C11-H18	1.0931	1.0860
C11-H19	1.0916	1.0839
C11-H20	1.0916	1.0846
C1-C2-C3	120.0344	120.0111
C1-C2-C7	120.0484	119.7447
C3-C2-C7	119.9172	120.2439
C2-C3-C4	119.0998	119.3294
C2-C3-O9	116.0511	120.2781
C4-C3-O9	124.8491	120.2781
C3-C4-C5	120.0296	120.119
C3-C4-H12	120.4138	118.7985
C5-C4-H12	119.5566	121.0771
C4-C5-C6	121.0884	120.6806
C4-C5-H13	118.971	119.4636
C6-C5-H13	119.9406	119.8548
C5-C6-C7	119.2682	119.4762
C5-C6-H14	120.5833	120.4438
C7-C6-H14	120.1485	120.0791
C2-C7-C6	120.5969	120.1499
C2-C7-H15	118.7015	119.2263
C6-C7-H15	120.7016	120.6233
C3-O9-C10	119.7013	116.8131
O9-C10-C11	107.4975	108.0322
O9-C10-H16	109.2973	109.0207
O9-C10-H17	109.2976	109.2888
C11-C10-H16	111.1187	111.2180
C11-C10-H17	111.1156	110.9133
H16-C10-H17	108.4846	108.3352
C10-C11-H18	109.7085	109.7467
C10-C11-H19	110.754	110.4459
C10-C11-H20	110.749	110.6651
H18-C11-H19	108.5529	108.6548
H18-C11-H20	108.5528	108.6195
H19-C11-H20	108.463	108.6572
C1-C2-C3-C4	-179.9953	-179.4858
C1-C2-C3-O9	0.008	-1.9206
C7-C2-C3-C4	0.0057	0.3139
C7-C2-C3-O9	180.009	177.8791
C1-C2-C7-C6	-180.0016	179.7599

C1-C2-C7-H15	-0.0015	0.0138
C3-C2-C7-C6	-0.0027	-0.0403
C3-C2-C7-H15	-180.0026	-179.7864
C2-C3-C4-C5	-0.0043	-0.3592
C2-C3-C4-H12	179.9912	178.7992
O9-C3-C4-C5	-180.0079	-177.9226
O9-C3-C4-H12	-0.0123	1.2357
C2-C3-O9-C10	-179.9783	180.6645
C4-C3-O9-C10	0.0252	0.1253
C3-C4-C5-C6	-0.0003	0.1329
C3-C4-C5-H13	179.9974	179.7671
H12-C4-C5-C6	-179.9958	-179.0059
H12-C4-C5-H13	0.0019	0.6282
C4-C5-C6-C7	0.0034	0.143
C4-C5-C6-H14	179.9984	179.7954
H13-C5-C6-C7	-179.9943	-179.4897
H13-C5-C6-H14	0.0007	0.1627
C5-C6-C7-C2	-0.019	-0.188
C5-C6-C7-H15	179.998	179.5545
H14-C6-C7-C2	-179.9969	-179.8417
H14-C6-C7-H15	0.003	-0.0991
C3-O9-C10-C11	-180.0167	-177.8527
C3-O9-C10-H16	59.276	61.162
C3-O9-C10-H17	-59.3129	-57.0789
O9-C10-C11-H18	180.0087	-179.7411
O9-C10-C11-H19	60.1953	60.4884
O9-C10-C11-H20	-60.1825	-59.8765
H16-C10-C11-H19	179.7473	-179.9041
H16-C10-C11-H20	59.3696	59.731
H17-C10-C11-H18	60.458	60.504
H17-C10-C11-H19	-59.3554	-59.2665
H17-C10-C11-H20	-179.7332	-179.6314

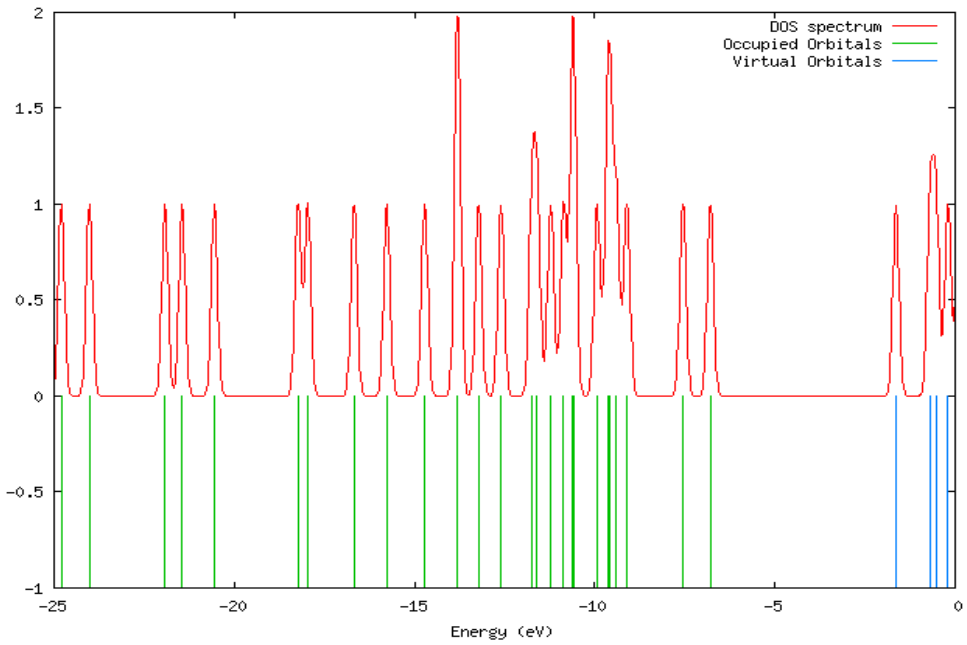

Fig. 2: The frontier molecular orbital energies and corresponding density of state (DOS) spectrum of the dye 2-Ethoxybenzonitrile

While the calculated HOMO and LUMO energies of the bare $Ti_{38}O_{76}$ cluster as a model for nanocrystalline are -6.55 and -2.77eV, respectively, resulting in a HOMO–LUMO gap of 3.78 eV, the lowest transition is reduced to 3.20 eV according

to TDDFT, and this value is slightly smaller than typical band gap of TiO_2 nanoparticles with nm size [44]. Furthermore, the HOMO, LUMO and HOMO–LUMO gap of $(TiO_2)_{60}$ cluster is -7.52, -2.97, and 4.55 eV (B3LYP/VDZ), respectively [45]. Taking into account of the cluster size effects and the calculated HOMO, LUMO, HOMO–LUMO gap of the dye 2-Ethoxybenzonitrile, $Ti_{38}O_{76}$ and $(TiO_2)_{60}$ clusters, we can find that the HOMO energies of these dyes fall within the TiO_2 gap.

The above data also reveal the interfacial electron transfer between semiconductor TiO_2 electrode and the dye sensitizer 2-Ethoxybenzonitrile is electron injection processes from excited dye to the semiconductor conduction band. This is a kind of typical interfacial electron transfer reaction[46].

3.3. Polarizability and hyperpolarizability

Polarizabilities and hyperpolarizabilities characterize the response of a system in an applied electric field[47]. They determine not only the strength of molecular interactions (long-range intermolecular induction, dispersion forces, etc.) as well as the cross sections of different scattering and collision processes, but also the nonlinear optical properties (NLO) of the system[48,49]. It has been found that the dye sensitizer hemicyanine system, which has high NLO property, usually possesses high photoelectric conversion performance[50]. In order to investigate the relationships among photocurrent generation, molecular structures and NLO, the polarizabilities and hyperpolarizabilities of 2-Ethoxybenzonitrile was calculated.

The polarizabilities and hyperpolarizabilities could be computed via finite field (FF) method, sum-over state (SOS) method based on TD-DFT, and coupled-perturbed HF (CPHF) method. However, the use of FF, SOS, and CPHF methods with large sized basis sets for 2-Ethoxybenzonitrile is too expensive. Here, the polarizability and the first hyperpolarizabilities are computed as a numerical derivative of the dipole moment using B3LYP/6-31G(d,p). The definitions [48,49] for the isotropic polarizability is

$$\alpha = \frac{1}{3}\left(\alpha_{XX} + \alpha_{YY} + \alpha_{ZZ}\right)$$

The polarizability anisotropy invariant is

$$\Delta\alpha = \left[\frac{\left(\alpha_{XX} - \alpha_{YY}\right)^2 + \left(\alpha_{YY} - \alpha_{ZZ}\right)^2 + \left(\alpha_{ZZ} - \alpha_{XX}\right)^2}{2}\right]^{\frac{1}{2}}$$

and the average hyperpolarizability is

$$\beta_{\square} = \frac{1}{5}\left(\beta_{iiZ} + \beta_{iZi} + \beta_{Zii}\right)$$

Where, α_{XX}, α_{YY}, and α_{ZZ} are tensor components of polarizability; β_{iiZ}, β_{iZi}, and β_{Zii} (i from X to Z) are tensor components of hyperpolarizability.

Table 2: Polarizability (α) of the dye 2-Ethoxybenzonitrile (in a.u.)

α_{xx}	α_{xy}	α_{yy}	α_{xz}	α_{yz}	α_{zz}	α	Δα
-52.5839	2.7209	-75.9576	-0.0750	-0.0589	-67.3757	-65.3057	14.4809

Table 3: Hyperpolarizability (β) of the dye 2-Ethoxybenzonitrile (in a.u.)

β_{xxx}	β_{xxy}	β_{xyy}	β_{yyy}	β_{xxz}	β_{xyz}	β_{yyz}	β_{xzz}	β_{yzz}	β_{zzz}	β_{ii}
-7.2677	-7.2765	0.6594	-75.7169	1.9625	-0.0173	1.0077	-10.4659	1.8996	0.8027	2.2637

Tables 2 and 3 list the values of the polarizabilities and hyperpolarizabilities of the dye 2-Ethoxybenzonitrile. In addition to the individual tensor components of the polarizabilties and the first hyperpolarizabilities, the isotropic polarizability, polarizability anisotropy invariant and hyperpolarizability are also calculated. The calculated isotropic polarizability of 2-Ethoxybenzonitrile -73.8781a.u. However, the calculated isotropic polarizability of JK16, JK17, dye 1, dye 2, D5, DST and DSS is 759.9, 1015.5, 694.7, 785.7, 510.6, 611.2 and 802.9 a.u., respectively [51,52]. The above data indicate that the donor-

conjugate p bridge-acceptor (D-p-A) chain-like dyes have stronger response for external electric field. Whereas, for dye sensitizers D5, DST, DSS, JK16, JK17, dye 1 and dye 2, on the basis of the published photo-to-current conversion efficiencies, the similarity and the difference of geometries, and the calculated isotropic polarizabilities, it is found that the longer the length of the conjugate bridge in similar dyes, the larger the polarizability of the dye molecule, and the lower the photo-to-current conversion efficiency. This may be due to the fact that the longer conjugate-p-bridge enlarged the delocalization of electrons, thus it enhanced the response of the external field, but the enlarged delocalization may be not favorable to generate charge separated state effectively. So it induces the lower photo-to-current conversion efficiency.

3.4. Electronic absorption spectra and sensitized mechanism

In order to understand the electronic transitions of 2-Ethoxybenzonitrile, TD-DFT calculations on electronic absorption spectra in vacuum and solvent were performed, and the results are shown in Fig. 3. It is observed that, for 2-Ethoxybenzonitrile, the absorption in the visible region is much weaker than that in the UV region. The calculated results have a red-shift. The results of TD-DFT have an appreciable red-shift, and the degree of red-shift in solvent is more significant than that in vacuum. The discrepancy between vacuum and solvent effects in TD-DFT calculations may result from two aspects. The first aspect is smaller gap of materials which induces smaller excited energies. The other is solvent effects. Measurements of electronic absorptions are usually performed in Solvent, especially polar solvent, could affect the geometry and electronic structure as well as the properties of molecules through the long-range interaction between solute molecule and solvent molecule. For these reasons it is more difficult to make the TD-DFT calculation is consistent with quantitatively. Though the discrepancy exists, the TD-DFT calculations are capable of describing the spectral features of 2-Ethoxybenzonitrile because of the agreement of lineshape and relative strength as compared with the vacuum and solvent.

The HOMO-LUMO gap of 2-Ethoxybenzonitrile in acetonitrile at B3LYP/6-31G (d,p) theory level is smaller than that in vacuum. This fact indicates that the solvent effects stabilize the frontier orbitals of 2-Ethoxybenzonitrile. So it induces the smaller intensities and red-shift of the absorption as compared with that in vacuum.

In order to obtain the microscopic information about the electronic transitions, the corresponding MO properties are checked. The absorption in visible and near-UV region is the most important region for photo-to-current conversion, so only the 20 lowest singlet/singlet transitions of the absorption band in visible and near-UV region for 2-Ethoxybenzonitrile is listed in Table 4. The data of Table 4 and Fig. 4 are based on the 6-311G (d,p) results with solvent effects involved.

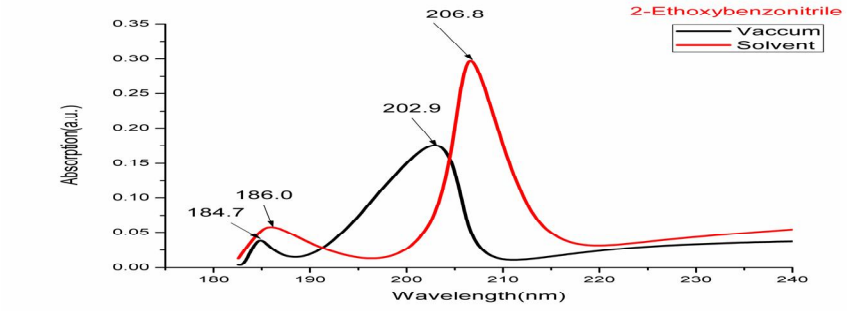

Fig. 3: Calculated electronic absorption spectra of the dye 2-Ethoxybenzonitrile

This indicates that the transitions are photo induced charge transfer processes, thus the excitations generate charge separated states, which should favour the electron injection from the excited dye to semiconductor surface.

The solar energy to electricity conversion efficiency (η) under AM 1.5 white-light irradiation can be obtained from the following formula:

$$\eta(\%) = \frac{J_{SC}[mAcm^{-2}]V_{OC}[V]\,ff}{I_0[mWcm^{-2}]} \times 100$$

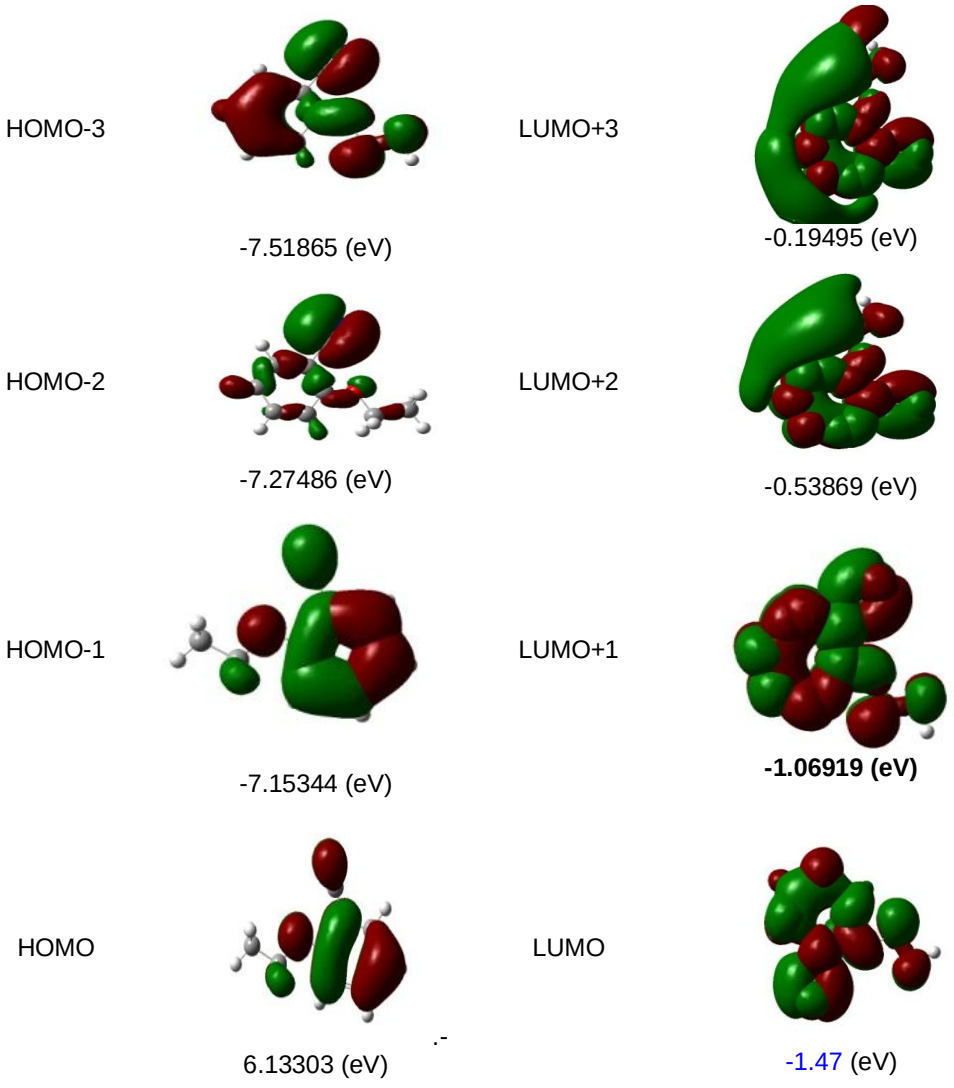

Fig. 4: Isodensity plots (isodensity contour = 0.02 a.u.) of the frontier orbitals of 2-Ethoxybenzonitrile

Where I_0 is the photon flux, J_{sc} is the short-circuit photocurrent density, and V_{oc} is the open-circuit photovoltage, and *ff* represents the fill factor[53]. At present, the

J_{sc}, the V_{oc}, and the *ff* are only obtained by experiment, the relationship among these quantities and the electronic structure of dye is still unknown. The analytical relationship between V_{oc} and E_{LUMO} may exist. According to the sensitized mechanism (electron injected from the excited dyes to the semiconductor conduction band) and single electron and single state approximation, there is an energy relationship:

Table 4: Computed excitation energies, electronic transition configurations and oscillator strengths (f) for the optical transitions with f > 0.01 of the absorption bands in visible and near-UV region for thedye 2-Ethoxybenzonitrile in acetonitrile

State	Configurations composition (corresponding transition orbitals)	Excitation energy (eV/nm)	oscillator strength (f)
1	0.37520 (34 → 36) 0.20199 (35 → 36)0.55763 (35 → 37)	5.0776 / 244.18	f=0.0107
2	-0.11538 (34 → 36) -0.20973 (34 → 37) 0.58944 (35 → 36) -0.18426 (35 → 37)	5.4523 / 227.40	f=0.2579
3	0.69986 (35 → 38)	5.8325 / 212.57	f=0.0064
4	0.69592 (35 → 39)	6.3217 / 196.12	f=0.0016
5	0.11750 (29 → 37) -0.17833 (33 → 37) 0.49686 (34 → 36) -0.14880 (34 → 37) -0.29665(35 → 37)	6.3637 / 194.83	f=0.2618
6	0.66178(35 → 40) 0.21690(35 → 41)	6.4111 / 193.39	f=0.0028
7	0.68348 (34 → 38) -0.12824 (34 → 39)	6.5747 / 188.58	f=0.0010
8	-0.10934 (29 → 36) 0.13654 (34 → 36) 0.55914 (34 → 37)0.15150 (35 → 36) -0.14560 (35 → 42)	6.6950 / 185.19	f=0.6552
9	-0.21825 (35 → 40) 0.65414 (35 → 41)	6.7629 / 183.33	f=0.0000
10	-0.36935(32 → 36) 0.45461 (35 → 44) 0.32959 (35 → 45)	6.9532 / 178.31	f=0.0000
11	0.11026 (34 → 37) 0.68550 (35 → 42)	6.9848 / 177.51	f=0.0045
12	0.55834 (32 → 36) -0.11581 (32 → 37) 0.11517 (34→ 39) 0.32082 (35 → 44) 0.19346 (35 → 45)	7.0141 / 176.76	f=0.0000
13	0.10330 (34 → 38) 0.63510 (34 → 39) 0.13941 (34→ 40) -0.17630 (35 → 43)	7.0457 / 175.97	f=0.0130
14	0.18908 (34 → 39) 0.66883 (35→ 43)	7.1208 / 174.12	f=0.0015
15	0.65820 (33 → 36)	7.1324 / 173.83	f=0.0432
16	-0.10435 (34 → 39 0.65048 (34 → 40) 0.17109 (34 → 41)	7.2236 / 171.64	f=0.0023
17	0.65794 (33 → 37) 0.10807 (34→ 36)	7.2924 / 170.02	f=0.0605
18	0.42405 (31 → 36) 0.12942 (31→ 37) 0.13675 (32 → 36) 0.41383 (32 → 37)-0.18481 (35 → 44) 0.20556 (35 → 45)	7.3036 / 169.76	f=0.0010
19	-0.22748 (31 → 36) -0.17273 (32 → 37) - 0.36090 (35 → 44) 0.51038 (35 → 45)	7.3124 / 169.55	f=0.0038
20	0.47057 (31 → 36) -0.28885 (31 → 37) -0.41387 (32→ 37)	7.3731 / 168.16	f=0.0004

$$eV_{oc} = E_{LUMO} - E_{CB}$$

Where, E_{CB} is the energy of the semiconductor's conduction band edge. So the V_{oc} may be obtained applying the following formula:

$$V_{oc} = \frac{(E_{LUMO} - E_{CB})}{e}$$

It induces that the higher the E_{LUMO}, the larger the V_{oc}. The results of organic dye sensitizer JK16 and JK17 [39], D-ST and D-SS also proved the tendency [54] (JK16: LUMO = -2.73 eV, V_{oc} = 0.74 V; JK17: LUMO = -2.87 eV, V_{oc} = 0.67 V; D-SS: LUMO = -2.91 eV, V_{oc} = 0.70 V; D-ST: LUMO = -2.83 eV, V_{oc} = 0.73 V). Certainly, this formula expects further test by experiment and theoretical calculation**.** The J_{sc} is determined by two processes, one is the rate of electron injection from the excited dyes to the conduction band of semiconductor, and the other is the rate of redox between the

excited dyes and electrolyte. Electrolyte effect on the redox processes is very complex, and it is not taken into account in the present calculations. This indicates that most of excited states of 2-Ethoxybenzonitrile have larger absorption coefficient, and then with shorter lifetime for the excited states, so it results in the higher electron injection rate which leads to the larger J_{sc} of 2-Ethoxybenzonitrile. On the basis of above analysis, it is clear that the 2-Ethoxybenzonitrile has better performance in DSSC.

4. CONCLUSIONS

The geometries, electronic structures, polarizabilities, and hyperpolarizabilities of dye 2-Ethoxybenzonitrile was studied by using ab initio HF and density functional theory with hybrid functional B3LYP, and the UV-Vis spectra were investigated by using TD-DFT methods. The NBO results suggest that 2-Ethoxybenzonitrile is a (D-p-A) system. The calculated isotropic polarizability of 2-Ethoxybenzonitrile is -73.8781 a.u. The calculated polarizability anisotropy invariant of 2-Ethoxybenzonitrile is 14.4767 a.u. The hyperpolarizability of 2-Ethoxybenzonitrile is 1.69587 a.u. The electronic absorption spectral features in visible and near-UV region were assigned based on the qualitative agreement to TD-DFT calculations. The absorptions are all ascribed to π→π* transition. The three excited states with the lowest excited energies of 2-Ethoxybenzonitrile is photoinduced electron transfer processes that contributes sensitization of photo-to-current conversion processes. The interfacial electron transfer between semiconductor TiO_2 electrode and dye sensitizer 2-Ethoxybenzonitrile is electron injection process from excited dye as donor to the semiconductor conduction band. Based on the analysis of geometries, electronic structures, and spectrum properties between 2-Ethoxybenzonitrile the role of nitro group is as follows: it enlarged the distance between electron donor group and semiconductor surface, and decreased the timescale of the electron injection rate, resulted in giving lower conversion efficiency. This indicates that the choice of the appropriate conjugate bridge in dye sensitizer is very important to improve the performance of DSSC.

ACKNOWLEDGEMENT

This work was partly financially supported by University Grants Commission, Govt. of India, New Delhi, within the Major Research Project scheme under the approval-cum-sanction No. F.No.34-5\2008(SR) & 34-1/TN/08.

REFERENCES

1. B. Li, L. Wang, B. Kang, P. Wang, Y. Qiu, Sol. Energy Mater. Sol. Cells 90 (2006) 549.
2. B. O'Regan, M. Gratzel, Nature 353 (1991) 737.
3. M. Gratzel, J. Photochem. Photobiol. C 4 (2003) 145.
4. M. Gratzel, J. Photochem. Photobiol. A 164 (2004) 3.
5. M.K. Nazeeruddin, C. Klein, P. Liska, M. Gratzel, Coord. Chem. Rev. 249 (2005) 1460.
6. T. Dittrich, B. Neumann, H. Tributsch, J. Phys. Chem. C 111 (2007) 2265.
7. X.Z. Liu, Y.H. Luo, H. Li, Y.Z. Fan, Z.X. Yu, Y. Lin, L.Q. Chen, Q.B. Meng, Chem. Commun. 27 (2007) 2847.
8. J.B. Xia, F.Y. Li, H. Yang, X.H. Li, C.H. Huang, J. Mater. Sci. 42 (2007) 6412.
9. M.X. Li, X.B. Zhou, H. Xia, H.X. Zhang, Q.J. Pan, T. Liu, H.G. Fu, C.C. Sun, Inorg. Chem.47 (2008) 2312.
10. E. Muller, P. Liska, N. Vlachopoulos, M. Gratzel, J. Am. Chem. Soc. 115 (1993) 6382.
11. M.K. Nazeeruddin, P. Pechy, T. Renouard, S.M. Zakeeruddin, R. Humphry-Baker, P. Comte, P. Liska, L. Cevey, E. Costa, V. Shklover, L. Spiccia, G.B. Deacon, C.A. Bignozzi, M. Gratzel, J. Am. Chem. Soc. 123 (2001) 1613.
12. M. Gratzel, Inorg. Chem. 44 (2005) 6841.
13. K. Hara, T. Sato, R. Katoh, A. Furube, Y. Ohga, A. Shinpo, S. Suga, K. Sayama, H.Sugihara, H.

Arakawa, J. Phys. Chem. B 107 (2003) 597.
14. X.H. Zhang, C. Li, W.B. Wang, X.X. Cheng, X.S. Wang, B.W. Zhang, J. Mater. Chem. 17(2007) 642 (and reference therein)
15. M. Liang, W. Xu, F. Cai, P. Chen, B. Peng, J. Chen, Z. Li, J. Phys. Chem. C 111 (2007)4465 (and reference therein).
16. W. Xu, B. Peng, J. Chen, M. Liang, F. Cai, J. Phys. Chem. C 112 (2008) 874.
17. F. De Angelis, S. Fantacci, A. Selloni, Chem. Phys. Lett. 389 (2004) 204.
18. F. De Angelis, S. Fantacci, A. Selloni, M.K. Nazeeruddin, Chem. Phys. Lett.415(2005)115.
19. Y. Xu, W.K. Chen, M.J. Cao, S.H. Liu, J.Q. Li, A.I. Philippopoulos, P. Falaras, Chem.Phys. 330 (2006) 204.
20. M.K. Nazeeruddin, F. De Angelis, S. Fantacci, A. Selloni, G. Viscardi, P. Liska, S. Ito, B. Takeru, M. Gratzel, J. Am. Chem. Soc. 127 (2005) 16835.
21. F. De Angelis, S. Fantacci, A. Selloni, M. Gratzel, M.K. Nazeeruddin, Nano. Lett.10 (2007) 3189.
22. F. De Angelis, S. Fantacci, A. Selloni, M.K. Nazeeruddin, M. Gratzel, J. Am. Chem.Soc. 129 (2007) 14156.
23. F. De Angelis, S. Fantacci, A. Selloni, Nanotechnology 19 (2008) 424002.
24. D. Di Censo, S. Fantacci, F. De Angelis, C. Klein, N. Evans, K. Kalyanasundaram, H.J. Bolink, M. Gratzel, M.K. Nazeeruddin, Inorg. Chem. 47 (2008) 980.
25. Y. Kurashige, T. Nakajima, S. Kurashige, K. Hirao, Y. Nishikitani, J. Phys. Chem. A111 (2007) 5544.
26. M.P. Balanay, D.H. Kim, Phys. Chem. Chem. Phys. 10 (2008) 5121.
27. P. Persson, M.J. Lundqvist, J. Phys. Chem. B 109 (2005) 11918.
28. P. Persson, M.J. Lundqvist, R. Ernstorfer, W.A. Goddard III, F. Willig, J. Chem.Theory Comput. 2 (2006) 441
29. M.J. Lundqvist, M. Nisling, S. Lunell, B. Akermark, P. Persson, J. Phys. Chem. B110 (2006) 20513.
30. M. Nilsing, P. Persson, S. Lunell, L. Ojamae, J. Phys. Chem. C 111 (2007) 12116.
31. W.R. Duncan, O.V. Prezhdo, Annu. Rev. Phys. Chem. 58 (2007) 143.
32. W.R. Duncan, O.V. Prezhdo, J. Am. Chem. Soc. 130 (2008) 9756.
33. L.G.C. Rego, V.S. Batista, J. Am. Chem. Soc. 125 (2003) 7989.
34. Z.Y. Guo, Y. Zhao, W.Z. Liang, G.H. Chen, J. Phys. Chem. C 112 (2008) 16655.
35. I. Kondov, M. Clzek, C. Benesch, H.B. Wang, M. Thoss, J. Phys. Chem. C 111 (2007) 11970
36. N. Robertson, Angew. Chem. Int. Ed. 45 (2006) 2338.
37. S. Ito, H. Miura, S. Uchida, M. Takata, K. Sumioka, P. Liska, P. Comte, P. Pechy, M.Gratzel, Chem. Commun. (2008), 5194-5196.
38. M.J. Frisch, G.W. Trucks, H.B. Schlegel, et al., Gaussian 03,Revision B.04. Gaussian, Inc., Pittsburgh, PA, 2003.
39. A.D. Becke, J. Chem. Phys. 98 (1993), 5648-5652.
40. B. Miehlich, A. Savin, H. Stoll, H. Preuss, Chem. Phys. Lett. 157 (1989), 200-206.
41. C. Lee, W. Yang, R.G. Parr, Phys. Rev. B. 37 (1988), 785-789.
42. V. Barone, M. Cossi, J. Phys. Chem. A 102 (1998), 1995-2001.
43. M. Cossi, N. Rega, G. Scalmani, V. Barone, J. Comput. Chem. 24 (2003), 669-681.
44. M.K. Nazeeruddin, F. De Angelis, S. Fantacci, A. Selloni, G. Viscardi, P. Liska, S.Ito, B.Takeru, M. Gratzel, J. Am. Chem. Soc. 127 (2005), 16835-16847.
45. M.J. Lundqvist, M. Nilsing, P. Persson, S. Lunell, Int. J. Quantum Chem. 106 (2006), 3214-3234
46. D.F. Waston, G.J. Meyer, Annu. Rev. Phys. Chem. 56 (2005), 119-156.

47. C. R. Zhang, H. S. Chen, and G. H. Wang, Chem. Res. Chin. U. 20 (2004), 640-646.
48. Y. Sun, X. Chen, L. Sun, X. Guo, W. Lu, Chem.Phys. Lett. 381 (2003), 397-403.
49. O. Christiansen, J. Gauss, J. F. Stanton, Chem.Phys. Lett. 305 (1999), 147-155.
50. Z. S. Wang, Y. Y. Huang, C. H. Huang, J. Zheng, H.M. Cheng, S. J. Tian, Synth. Met. 14 (2000), 201-207.
51. C.R. Zhang, Y.Z. Wu, Y.H. Chen, H.S. Chen, Acta Phys. Chim. Sin. 25 (2009), 53-60.
52. A. Seidl, A. Gorling, P. Vogl, J. A. Majewski, M. Levy, Phys. Rev. B 53 (1996), 3764-3774.
53. K. Hara, T. Sato, R. Katoh, A. Furube, Y. Ohga, A. Shinpo, S. Suga, K. Sayama, H.Sugihara, H. Arakawa, J. Phys. Chem. B. 107 (2003), 597-606.
54. C.R. Zhang, Z.J. Liu, Y.H. Chen, H.S. Chen, Y.Z. Wu, L.H. Yuan, J. Mol. Struct.(THEOCHEM) 899 (2009), 86-93.